Large magnetic resonance band gaps for split ring structures with high internal fractions

Ruey-Lin Chern

Institute of Applied Mechanics, National Taiwan University, Taipei 106, Taiwan, Republic of China

chern@iam.ntu.edu.tw

Abstract: The author investigates the characteristics of magnetic resonance band gaps for split ring structures. Resonance band gap width is related to the discrepancy of resonance frequency at two different Bloch wavelength scales. Large band gaps are achieved by lowering the resonance frequency on one hand, and raising the dissimilarity between two respective resonant modes on the other. By increasing the internal fraction of ring area, large resonance band gaps are obtained. The band gap features alter as the plasmonic effect becomes significant, where the kinetic inductance outweighs the geometric one and the magnetic resonance attenuates.

OCIS codes: (160.3918) Metamaterials; (160.4670) Optical materials; (260.5740) Resonance.

References and links

1. J. B. Pendry, A. J. Holden, D. J. Robbins, and W. J. Stewart, "Magnetism from conductors and enhanced nonlinear phenomena," IEEE Trans. Microw. Theory Tech. **47**, 2075–2084 (1999).
2. D. R. Smith and N. Kroll, "Negative Refractive Index in Left-Handed Materials," Phys. Rev. Lett. **85**, 2933–2936 (2000).
3. D. R. Smith, J. B. Pendry, and M. C. K. Wiltshire, "Metamaterials and Negative Refractive Index," Science **305**, 788–792 (2004).
4. T. J. Yen, W. J. Padilla, N. Fang, D. C. Vier, D. R. Smith, J. B. Pendry, D. N. Basov, and X. Zhang, "Terahertz Magnetic Response from Artificial Materials," Science **303**, 1494–1496 (2004).
5. S. Linden, C. Enkrich, M. Wegener, J. Zhou, T. Koschny, and C. M. Soukoulis, "Magnetic Response of Metamaterials at 100 Terahertz," Science **306**, 1351–1353 (2004).
6. H. Chen, L. Ran, J. Huangfu, T. M. Grzegorczyk, and J. A. Kong, "Equivalent circuit model for left-handed metamaterials," J. Appl. Phys. **100**, 024,915 (2006).
7. A. B. Movchan and S. Guenneau, "Split-ring resonators and localized modes," Phys. Rev. B **70**, 125,116 (2004).
8. Z. Liu, X. Zhang, Y. Mao, Y. Y. Zhu, Z. Yang, C. T. Chan, and P. Sheng, "Locally Resonant Sonic Materials," Science **289**, 1734–1736 (2000).
9. A. Moroz and A. Tip, "Resonance-induced effects in photonic crystals," J. Phys. Condens. Matter **11**, 2503–2512 (1999).
10. R. L. Chern, C. C. Chang, and C. C. Chang, "Interfacial operator approach to computing band structures for photonic crystals of polar materials," Phys. Rev. B **73**, 235,123 (2006).
11. R. L. Chern, C. C. Chang, and C. C. Chang, "Surface and bulk modes for periodic structures of negative index materials," Phys. Rev. B **74**, 155,101 (2006).
12. R. L. Chern, "Surface plasmon modes for periodic lattices of plasmonic hole waveguides," Phys. Rev. B **77**, 045,409 (2008).
13. R. A. Shelby, D. R. Smith, S. C. Nemat-Nasser, and S. Schultz, "Microwave transmission through a two-dimensional, isotropic, left-handed metamaterial," Appl. Phys. Lett. **78**, 489–491 (2001).
14. S. O'Brien and J. Pendry, "Magnetic activity at infrared frequencies in structured metallic photonic crystals," J. Phys.-Condes. Matter **14**, 6383–6394 (2002).
15. J. Zhou, T. Koschny, M. Kafesaki, E. N. Economou, J. B. Pendry, and C. M. Soukoulis, "Saturation of the Magnetic Response of Split-Ring Resonators at Optical Frequencies," Phys. Rev. Lett. **95**, 223,902 (2005).

#98860 - $15.00 USD Received 15 Jul 2008; revised 1 Nov 2008; accepted 14 Nov 2008; published 24 Nov 2008

16. R. L. Chern, "Magnetic and surface plasmon resonances for periodic lattices of plasmonic split-ring resonators," Phys. Rev. B **78**, 085,116.

1. Introduction

Split ring resonator (SRR) [1] has been the essential element in the design of metamaterials in recent years [2, 3]. Due to the adverse magnetic response [4, 5], SRR structures may in effect exhibit a negative permeability, which is not available in naturally occurring materials. This unusual property comes from resonance of fields within the SRR element, and can be described in terms of the equivalent circuit model [6]. An SRR element is understood as an electromagnetic analog of *LC* circuit, in which the ring acts as an inductor and the gap as a capacitor. As the time-varying magnetic field aligns parallel to the ring axis, currents and charges are induced on the metal surface. Near the resonance condition, the resultant field amplitude is strongly enhanced. Once the frequency goes above the resonance, the phase continues to lag behind until it is completely out of phase to the incident field. As a result, the magnetic response behaves in an adverse manner.

In order to seek for a large magnetic activity, a very inhomogeneous field distribution within the SRR element is required [1]. As a gap is brought into the ring to build a split ring configuration, the ring geometry becomes an open boundary instead of a closed one. An extra degree of freedom for field oscillation is introduced into the system, and the gap behaves like a defect [7]. Due to the concentration of energy within the SRR element, magnetic resonance for SRR structures occurs at a relatively lower frequency range. A similar feature appears for acoustic wave in the locally resonant sonic materials [8].

As the field is localized within individual SRR elements (with rather weak interactions between neighboring cells) when the magnetic resonance occurs, the propagation of field may be prohibited over a certain frequency range. In periodic structures, the local resonance is coupled to periodic scattering, resulting in a hybridization of Bragg and resonance bands [9]. Broadening of individual resonance thus leads to the formation of forbidden gaps in the dispersion diagram. For SRR structures, the resonance region can be effectively enlarged by making good use of the geometric property.

In this study, the author aims to explore the mechanism of magnetic resonance band gaps for SRR structures, and identify the features of large band gaps in terms of resonant modes. The interface matching method [10, 11, 12] is employed to solve the underlying problem, where the plasmonic effect is taken into account through the skin depth. The basic thinking for obtaining large resonance gaps is first to identify the key features of resonant modes at the upper and lower band edges, respectively, and then to raise the dissimilarity between the two respective modes so that the discrepancy of resonance frequency would be significant. By increasing the internal fraction of ring area, the band gap width as well as gap ratio can be substantially enlarged. In particular, the square SRR structure with large width and small thickness may possess a rather large band gap. The underlying mechanism is illustrated with the resonant mode patterns at the upper and lower band edges, which occur at two different Bloch wavelength scales. The present results are compared with the permeability model based on the effective medium theory [1] when the skin depth is negligible. As the plasmonic effect becomes significant, the band gap features alter due to the increasing importance of kinetic inductance and the attenuation of magnetic resonance.

#98860 - $15.00 USD Received 15 Jul 2008; revised 1 Nov 2008; accepted 14 Nov 2008; published 24 Nov 2008

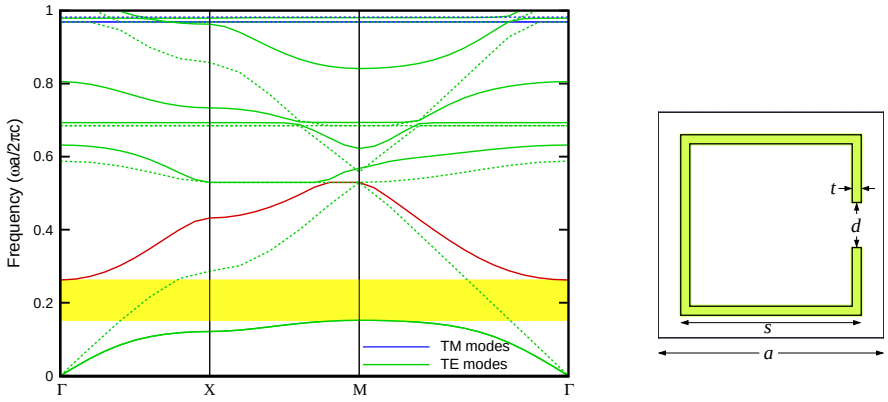

Fig. 1. Dispersion diagram for a square SRR structure with $s/a = 0.8$, $t/a = 0.04$, $d/a = 0.2$. Yellow region is the resonance band gap and dashed lines are results for a closed ring structure ($d = 0$) with the same s and t. The unit cell and geometric parameters are shown on the right.

2. Results and discussion

2.1. *Localized nature of magnetic resonance*

First, the case of vanishing skin depth $\delta_p \approx 0$ is considered for characterizing the magnetic resonance features that are solely determined by the geometry. Figure 1 shows the dispersion diagram for a square SRR structure with $s/a = 0.8$, $t/a = 0.04$, and $d/a = 0.2$. Magnetic resonance is characterized by a *resonance* frequency branch (in red color) for TE polarization, which is absent for a closed ring structure. For comparison, the results for $d = 0$ are overlaid in the same plot with dashed lines. This resonance branch appears between the two fundamental modes: acoustical and optical, where the acoustical (lower) branch begins with zero frequency and grows as the wave number increases, and the optical (higher) branch begins with a cutoff frequency and goes downward. A magnetic resonance band gap is opened immediately below the resonance branch. The upper band edge occurs at the Brillouin zone center (point Γ) on the resonance branch, while the lower edge locates at the zone edge (point M) on the acoustical branch.

The major feature of magnetic resonance is manifest on the mode patterns in terms of magnetic field vectors, as shown in Fig. 2 for a square SRR structure with $s/a = 0.5$, $t/a = 0.04$, and $d/a = 0.1$. A common feature is shared for the eigenmodes at both band edges: the fields are intense inside the SRR element, outside which the field amplitudes are substantially reduced and the field orientations are even reversed. This feature can be realized as being due to the *depolarization* field for a periodic structure with infinite extent [1]. The mode pattern in Fig. 2 also depicts a *localized* nature since the fields are strongly concentrated within the individual SRR element with rather weak interactions between neighboring cells. Localization prevents the field or energy from being transferred across the unit cell and indicates the existence of band gap.

The field patterns outside the SRR element exhibit a different feature. In Fig. 2(a), a *symmetric* pattern is shown in the region outside the SRR element, while Fig. 2(b) displays an *antisymmetric* distribution. This distinction is due to the phase change across the unit cell, according to

#98860 - $15.00 USD Received 15 Jul 2008; revised 1 Nov 2008; accepted 14 Nov 2008; published 24 Nov 2008

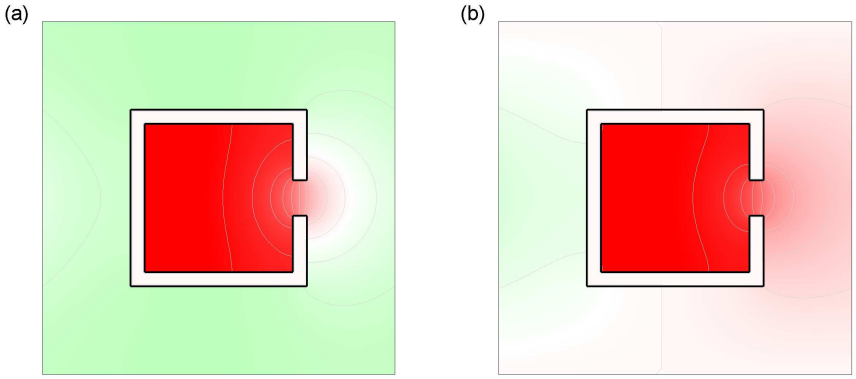

Fig. 2. Magnetic field contours (Re[**H**]) of the eigenmodes for a square SRR structure with $s/a = 0.5$, $t/a = 0.04$, and $d/a = 0.1$. Red and green colors correspond to positive and negative values, respectively. (a) the upper band edge: point Γ on the resonance branch with $\omega a/2\pi c = 0.304$. (b) the lower band edge: point M on the acoustical branch with $\omega a/2\pi c = 0.256$. The band gap width is $0.048(2\pi c/a)$ and the gap to mid-gap ratio is 17%.

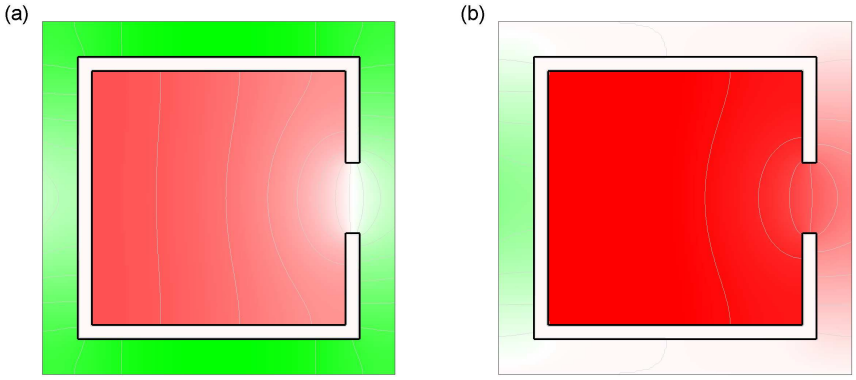

Fig. 3. Magnetic field contours (Re[**H**]) of the eigenmodes for a square SRR structure with $s/a = 0.8$, $t/a = 0.04$, $d/a = 0.2$ at (a) the upper band edge with $\omega a/2\pi c = 0.261$, and (b) the lower band edge with $\omega a/2\pi c = 0.151$. The band gap width is $0.11(2\pi c/a)$ and the gap to mid-gap ratio is 53.4%.

Bloch's theorem. Near the Brillouin zone edge (e.g. the point M), the Bloch wavelength is comparable to the unit cell size and the fields are out of phase to each other on opposing sides of the cell boundary. The difference in mode patterns accompanies a change of resonance frequency, which makes up the resonance band width.

2.2. Features of large resonance band gaps

A gap is associated with a resonance due to the coupling of individual resonance with the lattice scattering. The hybridization of Bragg and resonance bands leads to the broadening of individual resonance and the opening of band gaps [9]. For SRR structures, this feature was illustrated with the eigenmode patterns at two different Bloch wavelength scales (cf. Fig. 2).

#98860 - $15.00 USD Received 15 Jul 2008; revised 1 Nov 2008; accepted 14 Nov 2008; published 24 Nov 2008

By raising the *dissimilarity* between two respective eigenmodes, the resonance region can be enlarged as well. This is attained by increasing the internal fraction of ring area or, equivalently, reducing the portion outside the ring. Figure 3 shows the eigenmode patterns for a square SRR structure with a larger internal fraction ($s/a = 0.8, t/a = 0.04, d/a = 0.2$). As the region allowed for field variation (outside the ring) becomes smaller, the dissimilarity between Fig. 3(a) and (b) becomes more evident. Note that the resonant frequency at the upper band edge is slightly decreased, whereas the frequency at the lower band edge is greatly reduced. Accordingly, a substantially enlarged band gap width [from $0.048(2\pi c/a)$ to $0.11(2\pi c/a)$] and gap to mid-gap ratio (from 17% to 53.4%) are obtained.

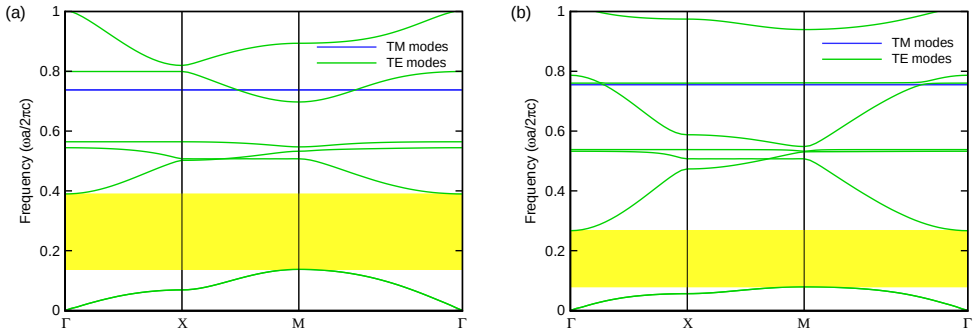

Fig. 4. Dispersion diagrams for the square SRR structures with $s/a = 0.95$ and $t/a = 0.01$. (a) the optimal band gap width $0.252(2\pi c/a)$ at $d/a = 0.85$, (b) the optimal gap to mid-gap ratio 109% at $d/a = 0.2$.

As the internal fraction of ring area is further increased, the band gap size can be even larger. Figure 4 shows the dispersion diagrams for SRR structures with a rather large width $s/a = 0.95$ and small thickness $t/a = 0.01$. In Fig. 4(a), an optimal band gap width $0.252(2\pi c/a)$ is attained at a large gap distance $d/a = 0.85$, and in Fig. 4(b), an optimal gap to mid-gap ratio 109% is achieved at a small gap distance $d/a = 0.2$. It is noticed that the resonance frequency at the lower band edge is substantially reduced [$0.138(2\pi c/a)$ and $0.079(2\pi c/a)$ in Fig. 4(a) and (b), respectively]. This is due to a large equivalent inductance L associated with a high fraction of internal area. For a small gap distance, the equivalent capacitance C is also large and the resonance frequency is even lower [cf. Fig. 4(b)].

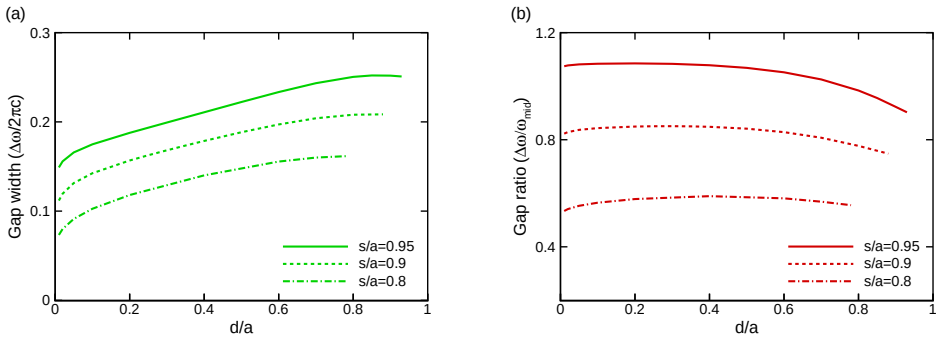

Fig. 5. Band gap widths and gap to mid-gap ratios of the SRR structures with $t/a = 0.01$ for various d/a and s/a.

#98860 - $15.00 USD Received 15 Jul 2008; revised 1 Nov 2008; accepted 14 Nov 2008; published 24 Nov 2008

The ring gap distance serves as another important geometric parameter that affects the band gap size. Since the gap is a passage between the inner and outer regions of the SRR element, a large gap distance may further raise the dissimilarity of resonant mode patterns between the two band edges. In Fig. 5, the band gap widths and gap to mid-gap ratios are plotted for various gap distances. It is shown that the optimal band gap width tends to occur at a large gap distance. On the other hand, the optimal gap to mid-gap ratio is likely to occur at a small gap distance, where the resonance frequency is lower due to a larger equivalent capacitance.

2.3. Effect of the internal fraction

The basic feature of magnetic resonance band gap for SRR structures can be related to the internal fraction through the effective permeability. According to the effective medium theory [1], a periodic array of SRR elements can be regarded as a homogeneous medium having the effective permeability

$$\mu_{\text{eff}} = 1 - \frac{F\omega^2}{\omega^2 - \omega_0^2}, \tag{1}$$

at the long wavelength, where ω_0 is the resonance frequency of the equivalent *LC* circuit and F is the internal fraction of ring area. Based on this permeability model, $\mu_{\text{eff}} < 0$ in the range $\omega_0 < \omega < \omega_m$, where $\omega_m = \omega_0/\sqrt{1-F}$ is considered as the *magnetic plasma frequency* for SRR structures [1, 13]. In principle, this frequency range would be the forbidden region in the dispersion diagram, in which ω_0 and ω_m correspond to the upper and lower bounds of magnetic resonance, respectively. As the fraction F is increased, the lower bound ω_0 is reduced due to a larger equivalent inductance L for a bigger ring ($\omega_0 \propto 1/\sqrt{L}$), provided that the ring gap distance remains unchanged. On the other hand, the upper bound ω_m does not have a marked change since both ω_0 and $\sqrt{1-F}$ are reduced as F increases. As a result, the resonance range $\Delta\omega = \omega_m - \omega_0$ would be significant for a large F.

The effective permeability characterizes the trend of magnetic resonance band gap with respect to the internal fraction, which is consistent with the dissimilarity of eigenmode patterns between the upper and lower band edges, as addressed in the previous subsection. Note, however, that the validity of effective permeability is restricted to a relatively low frequency range. For larger internal fractions, the lower limit of magnetic resonance tends to occur at even lower frequencies, whereas the upper limit may exceed what is supposed to be valid to a certain extent. In this situation, the actual value of effective permeability should be carefully examined.

2.4. Effect of the kinetic inductance

If the skin depth $\delta_p \equiv c/\omega_p$ is much smaller than the SRR size, magnetic resonance is solely determined by the SRR geometry. As the skin depth becomes comparable to or even larger than the SRR element, the kinetic energy of free electrons increases its importance and the magnetic resonance features begin to change. For a plasmonic SRR element, the equivalent inductance consists of two parts: $L = L_m + L_e$. The geometrical inductance (per unit length) $L_m = \mu_0(s-2t)^2$ is determined by the internal ring area [14], while the kinetic inductance (per unit length) $L_e = l/(t\varepsilon_0\omega_p^2) = \mu_o l c^2/(t\omega_p^2)$ comes from the free electron motion [15], where $l = 4(s-t) - d$ is the circumference of the SRR element. It follows that $L_m \propto a^2$ and $L_e \propto \delta_p^2$. Meanwhile, the equivalent capacitance (per unit length) $C = \varepsilon_0 t/d$ remains unchanged for different a and δ_p.

For $\delta_p \ll a$, $\omega_0 = 1/\sqrt{LC} \propto 1/a$ is reciprocally scaled with the lattice period. For $\delta_p \gg a$, on the other hand, $\omega_0 \propto 1/\delta_p$ is inversely proportional to the skin depth. In this situation, the kinetic inductance L_e outweighs the geometric inductance L_m, and the magnetic resonance frequency tends to saturate [15, 16]. This feature is accompanied with the diminishing of localized nature

#98860 - $15.00 USD Received 15 Jul 2008; revised 1 Nov 2008; accepted 14 Nov 2008; published 24 Nov 2008

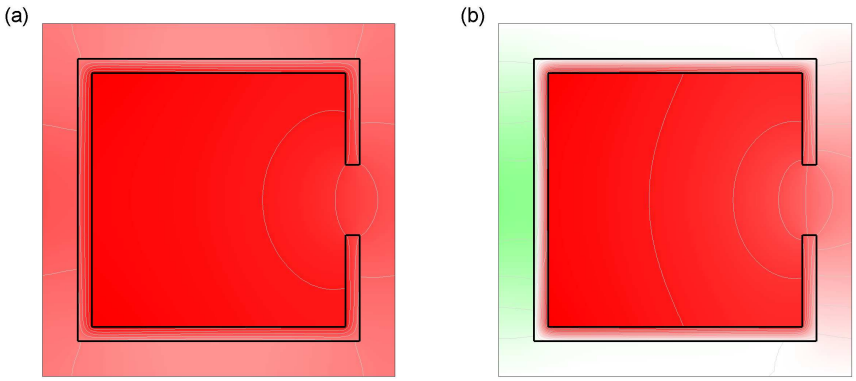

Fig. 6. Magnetic field contours (Re[**H**]) of the eigenmodes for the SRR structure in Fig. 3 with $\delta_p/a = 1$ at (a) the upper band edge and (b) the lower band edge.

in the eigenmode pattern, as shown in Fig. 6(a), where the fields between inside and outside the ring no longer exhibits a large contrast as in Fig. 3 for $\delta_p \approx 0$. The magnetic resonance is thus attenuated. On the other hand, the mode pattern in Fig. 6(b) is less affected by the skin depth as the Bragg resonance dominates the characteristics of magnetic resonance at the Brilloun zone edge. Nevertheless, the resonance frequency is substantially changed [16].

3. Concluding remarks

In conclusion, basic features of magnetic resonance band gaps for split ring structures were investigated, with emphasis on the dispersion characteristics. The internal fraction of ring area is a key factor for obtaining large magnetic resonance band gaps. A square SRR structure with large width and small thickness ($s/a = 0.95$ and $t/a = 0.01$) would give rise to a large band gap width [$0.252(2\pi c/a)$] as well as large gap ratio (109%). This feature can be understood by the raised dissimilarity of resonant mode patterns between the upper and lower band edges. In terms of the effective permeability, the present results shows consistency with the effective medium theory for negligible skin depths. As the plasmonic effect increases its importance for sizable skin depths, the band gap features exhibit a notable change due to the kinetic energy of free electrons. For sufficiently large skin depth, the kinetic inductance outweighs the geometric one and the magnetic resonance attenuates.

Acknowledgments

This work was supported in part by National Science Council of the Republic of China under Contract No. NSC 96-2221-E-002-190-MY3 and NSC 97-2120-M-002-013.

#98860 - $15.00 USD Received 15 Jul 2008; revised 1 Nov 2008; accepted 14 Nov 2008; published 24 Nov 2008